Volume Shrinkage Dependence of Ferromagnetic Moment in the Lanthanide Ferromagnets **Gadolinium, Terbium, Dysprosium, and Holmium**

Masaki Mito[1,*], Kazuya Matsumoto[1], Yuki Komorida[1], Hiroyuki Deguchi[1], Seishi Takagi[1], Takayuki Tajiri[2], Tomoharu Iwamoto[3], Tatsuya Kawae[3], Masahiko Tokita[4] and Kazuyoshi Takeda[3]

[1] *Faculty of Engineering, Kyushu Institute of Technology, Kitakyushu 804-8550, Japan*

[2] *Faculty of Science, Fukuoka University, Fukuoka 814-0180, Japan*

[3] *Department of Applied Quantum Physics, Kyushu University, Fukuoka 812-8581, Japan*

[4] *Faculty of Engineering, Fukuoka Institute of Technology, Fukuoka 811-0295, Japan*

<Abstract>

The Gd-Ho series of lanthanide ferromagnets, which includes gadolinium (Gd), terbium (Tb), dysprosium (Dy), and holmium (Ho), undergoes similar structural transitions, e.g., the hcp → Sm-type→ dhcp → fcc transitions, under pressure. Through high-field DC magnetic measurements and structural analyses, we found that the ferromagnetic moments disappeared at a specified critical pressure, which resulted in volume shrinkage of $16.7 \pm 1.7\%$ for each ferromagnet. The results of the present study suggest that the disappearance of the ferromagnetic moments of Gd-Ho under pressure could be understood within the framework of a band picture related to volume shrinkage.

PACS: 75.30.Cr, 75.50.Cc, 81.40.Vw, 75.10.Lp

Keywords: A. elements; A. magnetic materials; C. high pressure; D. magnetic properties; D. crystal structure

*corresponding author

Masaki Mito

1-1 Sensui-cho, Tobata-ku, Kitakyushu, 804-8550, JAPAN

tel&fax. ;81-93-884-3286

e-mail: mitoh@tobata.isc.kyutech.ac.jp

<Text>

1 Introduction

In the Periodic Table of the elements, single-element lanthanide ferromagnets based on gadolinium (Gd), terbium (Tb), dysprosium (Dy), and holmium (Ho) are representative single-element ferromagnets, together with the three transition metals of iron (Fe), cobalt (Co), and nickel (Ni). Experimental and theoretical studies have been actively facilitated by recent high-quality sample syntheses and advances in the theoretical calculations. The magnetic properties of the lanthanide series are mainly characterized by the localized 4f electrons, the charge clouds of which are located near the nuclei. This localization prevents the 4f electrons from participating in chemical bonding between the atoms. The valence electrons, with the exception of the 4f electrons, hybridize with those of the nearest neighboring atoms. The magnetic correlation between the 4f moments is characterized by the Ruderman-Kittel-Kasuya-Yosida (RKKY) interaction [1] *via* the conduction electron on the conduction band. In the case of Gd, it is known that the partially filled 5d/6s conduction bands also influence the magnitude of the magnetic moment, due to interband exchange coupling between itinerant band electrons and localized 4f electrons. The single-element lanthanide ferromagnets, with the exception of Gd, undergo both antiferromagnetic (AFM) and ferromagnetic (FM) transitions, and a helical magnetic structure with temperature-dependent helical angle is stabilized in the AFM region, $T_C < T < T_N$, in which the AFM and FM transition temperatures are defined as T_N and T_C, respectively. The crystal structures of four single-element ferromagnets, Gd-Ho, at ambient pressure are commonly hexagonal-closed-packaged (hcp) structures. It is well-known that a series of structural transitions, e.g., hcp → Sm-type → double hcp (dhcp) → face-centered-cubic (fcc) structures, appears under pressure conditions [2-6]. An overview is presented in Figure 1 [6]. Given three hexagonal planes A, B, and C, the stacking of the hcp structure is expressed as ABA, the Sm-type structure is ABABCBCACA, the dhcp

structure is ABACA, and the fcc structure is ABCA. Both the hcp and fcc structures are highest-occupied packing structures. From the viewpoint of stacking form, the Sm-type structure is considered to be a mixed structure of one-third fcc and two-thirds hcp, while the dhcp structure is half fcc and half hcp. This interpretation suggests that pressurization gradually increases the percentage of fcc in the entire crystal. To date, the magneto-structural correlation of Gd-Ho under pressure has been assumed to be closely related to the change in structural symmetry, whereas we believe that it is not sufficient to focus exclusively on structural symmetry to achieve an understanding of the magnetic properties under pressure. In the current paper, we propose that the key factor that characterizes the stability of the FM state is not structural symmetry, but rather volume shrinkage, based on the experimental evidence.

The magnetic properties [7, 8] and crystal structures [2-6] of Gd-Ho under pressure have been investigated by many groups. In particular, the structural analyses are complete. For instance, in the case of Gd, a series of structural transitions, e.g., hcp $\rightarrow$ Sm-type $\rightarrow$ dhcp $\rightarrow$ fcc $\rightarrow$ trigonal structures, have been reported at $P_{\text{hcp-Sm}} = 1.5 \pm 0.2$ GPa, $P_{\text{Sm-dhcp}} = 6.5 \pm 0.5$ GPa, $P_{\text{dhcp-fcc}} = 24.0\text{-}29.0$, and $P_{\text{fcc-trigonal}} = 44.0\text{-}55.0$ GPa, respectively [5]. However, regarding magnetic measurements, previous studies using the washer-shaped sample of a large volume encountered the problem of stress distribution [7, 8]. The appearance of magnetic anomalies suggests the splitting of magnetic transitions above a certain pressure. We assume that the AC susceptibility with multi-split anomalies detects a multi-domain structure, due to the inhomogeneity of the large sample. This may reflect a change in magnetic anisotropy under pressure, mentioned via the torque measurement in Gd [9]. Using high-field DC susceptibility measurement of Gd with a diamond anvil cell (DAC) and a superconducting quantum interference device (SQUID) magnetometer, we have shown previously that the FM transition of Gd does not split [10]. Subsequently, Jackson et al. used DAC to perform AC susceptibility measurements of Gd-Er, and they verified the systematic pressure

dependence of T_C and T_N in the absence of splitting. Furthermore, they have recently reported that the transition temperature is scaled as pressure, is normalized by a critical pressure [11]. On the theoretical aspect, Henemann and Temmerman have predicted the existence of a FM to AFM phase transition at 4-5 GPa for the hcp phase of Gd [12], which is attributed to reduced 4f localization. However, the mechanism underlying the disappearance of the FM moment in a series of single-element lanthanide ferromagnets (Gd-Ho) has not been studied systematically. Indeed, owing to technical problems with the experiments, magnetic measurements of Gd-Ho in high magnetic fields have not been undertaken in the GPa pressure range, and the experimental data obtained have not been sufficient for comprehensive discussions on the disappearance of these FM moments. In the current paper, we present important experimental data in relation to the mechanism underlying the instability of single-element lanthanide ferromagnets under pressure; these data have been generated using high-field DC magnetic measurements and powdered X-ray diffraction (XRD). In addition, we show that the disappearance of the Gd-Ho FM moments occurs when the volume shrinkage is approximately 17%, so that the disappearance of the FM moment could be explained by an effective band picture that involves the ratio of shrinkage of the unit cell volume. Thus, we elucidate the magnetic properties on single-element lanthanide ferromagnets under pressure.

2 Experimental

Polycrystalline samples of Gd, Tb, Dy, and Ho metals of high purity (99.9%) were purchased from Nippon Yttrium Co., Ltd. We measured the magnetization (M) levels in a high magnetic field (H) using the SQUID magnetometer (Quantum Design MPMS). Figure 2 shows the M-H curves for polycrystalline samples of the four lanthanide ferromagnets at T = 5 K. The external magnetic field of H = 0.3 T was sufficient to induce large proportions of the magnetic moments along the applied field direction, which resulted in fading of the

anisotropy effect discussed in the previous section. For instance, the magnetization of Gd at $H = 0.5$ T generated up to 73% of the saturated moment at ambient pressure. We estimated that a magnetic field of 0.3 T or 0.5 T would give sufficient information to evaluate quantitatively the FM moment. Pressures of up to 10 GPa were applied with a miniature DAC that was designed for the SQUID magnetometer. The details of the miniature DAC are described elsewhere [13, 14]. The pressure levels were calibrated using the ruby fluorescence method at room temperature [15]. Upon cooling of the miniature DAC, the pressure increase in relation to cooling to the temperature of liquid helium was estimated as being approximately 10% of the pressure estimated at room temperature [13]. The diamonds had flat tips of diameter 0.6 mm. The gasket was made of hardened, 0.2-mm-thick CuBe. In a sample cavity of diameter 0.2 mm, which was created in the gasket, a sample of about 30 μg and some pieces of ruby were contained in a pressure-transmitting medium, which consisted of a methanol:ethanol:water (16:3:1) mixture. In the DC measurement using MPMS, at any field strength, it is difficult to obtain the symmetric SQUID voltage against a cell transport of 4 cm in the coil system, since the contribution of a DAC made of CuBe in terms of magnetic response is very large. Thus, an appropriate amount of Co powder was mounted on the gasket using the insulating varnish GE-7031. Using this CuBe-Co composite gasket, we were able to maintain an ideal scanning response for the SQUID voltage over a wide temperature range in magnetic fields of 0.3-0.5 T [14]. Given that measurement accuracy was guaranteed, the temperature dependence of a small magnetic response of the measured sample could be evaluated. The values of T_C and T_N for Gd-Ho, which were estimated based on the change of curvature of $M(T)$, were consistent with those estimated by Jackson *et al*. [11]. As for Gd, Tb, and Dy, the powdered XRD patterns of the specimens used in the magnetic measurement were observed in a pressure range up to 13.3 GPa at room temperature using a synchrotron radiation X-ray powder diffractometer with a cylindrical imaging plate at the Photon Factory [Institute of Material Structure Science, High Energy Accelerator Research Organization (KEK)] [16]. The wavelength of the incident X-

ray was 0.6882(5) Å. The design of the DAC used in the present study was essentially to the same as that used for the magnetic measurements. We confirmed the structural transformations of the above three elements under pressure; the results were consistent with previous experimental results reported by different groups [2-6, 17].

3 Experimental results

3.1 Magnetic measurements

Figure 3(a)-(d) shows the temperature dependence of magnetization (M) for Gd-Ho under pressure. The background contribution attributed to DAC has been subtracted from the total signal.

Gadolinium

For Gd, triplicate measurements were performed at $H = 0.5$ T; the results from the third run are shown in Figure 3(a). At ambient pressure, the rapid development of M at temperatures below 300 K revealed the onset of FM ordering. In Figure 3(a), the FM ordering temperature T_C, which was assigned at ambient pressure, is represented by an arrow. With increasing pressure, the rapid development of M shifted towards the low-temperature side, while the maximum value of M at low temperatures, M_{max}, hardly changed in the initial pressure region below 2.6 GPa. However, M_{max} began to decrease rapidly across the critical pressure range of 2.6 to 3.8 GPa. At around $P = 7.5$ GPa, the FM character could not be confirmed. From the three runs, we conclude that the FM behavior survives at $P \leq 5.5$ GPa, whereas the magnitude of M begins to decrease at around $P = 2.6$ GPa. It is noteworthy that at a pressure of about 2 GPa, the hcp-Sm structural transition occurred. The Sm element magnet itself exhibits the AFM property.

In Gd, the hcp-Sm structural transition should trigger a decrease of the magnetic moment, as mentioned above, although is not associated unambiguously with the stabilization of the AFM state. It seems likely that the FM domains with the hcp structure survive even in the state characterized as the Sm-phase. Figure 4 shows the pressure dependence of T_C for Gd, together with the T_C and T_N for the other three ferromagnets. Furthermore, around $P = 9$ GPa, the dhcp transition was stabilized, as discussed below. The present experimental results indicate that the magnetic form in the dhcp state is certainly not FM. Thus, the present measurement in a high magnetic field of 0.5 T suggests that the transformation of the magnetic phase form the FM state to the AFM or paramagnetic (PM) state almost occurs at around $P = 7.5$ GPa. In a theoretical calculation of the hcp phase of Gd, Henemann and Temmerman have predicted that the FM to AFM phase transition occurs around 4-5 GPa [12]. These authors mentioned that the Sm structure corresponds to the metastable AFM structure [12]. Our experimental results are generally consistent with the above theoretical description.

Terbium

Tb originally has both the FM and AFM transitions within a narrow temperature range of 220-230 K, and it proved difficult to identify the AFM transition using DC measurement at $H = 0.5$ T. Thus, measurement at $H = 0.3$ T and two runs at $H = 0.5$ T were performed. Figure 3(b) shows the results of the third run at $H = 0.3$ T. At ambient pressure, we found two kinks of M at around 219 K (Fig. 3(b)). Comparison with the literature [18] reveals that the former position corresponds to T_C, while the latter corresponds to T_N. As the pressure increased, both T_C and T_N decreased. When the pressure exceeded 4 GPa, the FM signal was less than 10% of the initial level. As we describe below, at $P = 4.6 \pm 0.5$ GPa, the hcp-Sm transition occurred. In the case of Tb, disappearance of the FM moment seems to be closely connected with the hcp-Sm transition, in contrast to what was observed for Gd.

Dysprosium

For Dy, two DC measurements were performed at $H = 0.5$ T and $H = 0.3$ T. The experimental data for the second run at $H = 0.3$ T are shown in Figure 3(c). When the DC field was applied along the easy plane of the single crystal, a distinct increase in M due to a first-order transition was observed at T_C 90 K. However, the sample used in the present measurements was polycrystalline, and the FM ordering response was broad. In this instance, T_C was defined as the temperature of the uppermost position of the broad hump. As the DC field increased, the decrease in M below T_C was suppressed, and the hump due to the FM order was diminished. In this case, measurement at $H = 0.3$ T (rather than at $H = 0.5$ T) was adequate for determining T_C. The T_C and T_N values for Dy under pressure differed significantly, and T_C and T_N could be extrapolated with confidence over a wide pressure range, as compared to the analyses of Tb. In similarity to Tb, the disappearance of the FM moment of Dy occurred at a pressure that was slightly higher than the hcp-Sm transition pressure (see Fig. 4).

Holmium

For Ho, the T_C and T_N values were lower than those for Gd, Tb, and Dy. The experimental data from the second run at $H = 0.5$ T are shown in Figure 3(d). The magnitude of magnetization related to AFM ordering scarcely changed, even when T_N markedly decreased with increasing pressure. In contrast, the magnetic response of the FM ordering systematically decreased with increasing pressure. At pressures up to $P = 7.3$ GPa, both T_C and T_N could be determined (Fig. 4). The temperature dependence of M at $P = 9.2$ GPa (structurally, the Sm-type phase) for Ho was different from those at $P \leq 7.3$ GPa, and resembled that of Sm. The present result reveals that the hcp-Sm structural transition can be confirmed via magnetic measurement.

Figure 4 shows the FM and AFM transition temperatures, T_C and T_N, for Gd, Tb, Dy, and Ho. In the case of Gd, it was difficult to estimate T_C for $P > 5.5$ GPa, as shown in Figure 3(a). The T_C decreased in a linear fashion against pressure as d T_C /d$P = - 12.2$ K/GPa, which is consistent with the result obtained by Jackson et al. [11]. Jackson et al. did not determine T_N for Tb and T_C for Ho, whereas the current results represent the pressure dependencies of both T_C and T_N for Tb, Dy, and Ho; in other respects, the present results are essentially consistent with the previous report of Jackson et al. [11]. The values of the pressure gradients of T_C and T_N for Gd, Tb, Dy, and Ho are listed in Table 1.

Figure 5 shows the pressure dependence of the maximum value of $M(T)$ at $H = 0.3$ or 0.5 T, M_{max}, for the Gd-Ho series.   For instance, in Gd, the magnitude of M_{max} rapidly decreased at around 2.5 GPa, and was negligible at around 9.0 GPa. However, for $P >$ 6.5 GPa, the magnetic field of $H = 0.5$ T induced only a slight magnetic moment, corresponding to about 7% of the M_{max} at ambient pressure. A series of measurements were carried out at $H = 0.3$ T and 0.5 T, which was found to be sufficient to induce potent magnetization in the case of ferromagnets. Given the self-consistent LMTO calculations made by Henemann and Temmerman [12], we assume that the FM to AFM transition advances around $P = 2.5$ GPa, and at approximately $P = 7.5$ GPa, the AFM ordered state is stabilized. The present experimental system using a sample of mass < 0.01 mg does not sufficient sensitivity to allow observations of the AFM feature. Similar pressure-induced suppression of the magnetic signal has been reported by Robinson et al., who indicated the possibility of an FM to AFM transition at around 2.0-2.7 GPa [7]. However, our measurement at high magnetic fields gave more reliable results for determination of the critical pressure at which the FM moment disappears. In the present study, we have determined the critical pressure P_C for the Gd-Ho series, based of the results shown in Figure 5 and Table 1.

3.2 Structural Analyses

We investigated the crystal structures of Gd, Tb, and Dy under pressure, so as to confirm that the structural transformations described in the literature actually occurred in the present samples. The powdered XRD analyses were performed at room temperature in the following pressure regions: up to 13.3 GPa for Gd; up to 5.1 GPa for Tb; and up to 4.3 GPa for Dy.

First, let us explain the XRD data for Gd shown in Figure 6(a). The purple data represent the background data in the situation without the sample, and the huge anomaly visible at around $2\theta = 19\text{-}20°$ is a diffraction peak due to the gasket, which is made of CuBe. The predominant peaks, with the exception of the background peak, at ambient pressure are labeled by the plane index for the hcp structure, with $a = 3.653$ Å and $c = 5.794$ Å ($c/a = 1.586$). Three peaks, indexed as (100), (002), and (101), of the hcp structure appear at around $2\theta = 12\text{-}15°$. At the right side of the (100) peak, there is a supplementary anomaly that is marked with a blue, open, inverse triangle, corresponding to the (102) peak of the Sm type [17], which has also been described by Jayaraman and Sherwood [2]. This reveals that the Sm structure exists in a metastable state in a part of the present virgin sample of Gd. We examined the diffraction of the (102) plane at around $2\theta = 18.5°$, to recognize the disappearance of the hcp phase, since the Sm structure does not permit any diffraction at the corresponding angle [8]. Indeed, in the pressure region up to 2.6 GPa, the (102) peak survived, shifting towards the high-angle side, whereas at $P = 3.7$ GPa, this peak symbolic of hcp was hardly seen. Furthermore, the ratios of the unit cell volume to the initial volume within the pressure range of 1.5-3.7 GPa were as follows: $96.8 \pm 0.2\%$ at 1.5 GPa; $97.6 \pm 0.3\%$ at 2.0 GPa; $96.4 \pm 0.3\%$ at 2.6 GPa; and $94.5 \pm 0.3\%$ at 3.7 GPa. There was a small discontinuity of about 1% in volume shrinkage just above $P = 2.0$ GPa, which suggests that the Sm

phase begins to predominate at about 2.0 ± 0.5 GPa. Similar results have been reported previously [3].

Next, for $P > 8.0$ GPa, a new diffraction peak, which is due to the dhcp structure, marked with a blue, closed, inverse triangle, corresponding to the (101) peak of the dhcp structure [17], appears between peaks marked with blue or red open, inverse, triangles. This suggests that the dhcp structure becomes stabilized at pressures of around 9.0 GPa, instead of the Sm structure. After releasing the pressure of 13.3 GPa, the diffraction pattern almost recovered to the initial pattern, whereas the region of the metastable Sm-type domain appeared to be more enlarged than that of the initial state.

The structural analysis of Tb up to $P = 5.1$ GPa (Fig. 6(b)) shows that the diffraction of the (102) plane, which represents the hcp structure, disappears at $P = 5.1$ GPa, and that the diffraction pattern at around $2\theta = 13\text{-}15°$ is quite similar to that of Gd at $P = 2.6$ GPa. Therefore, we conclude that stabilization of the Sm-type structure occurs within the range of $P = 4.0\text{–}5.1$ GPa. This is consistent with the structural transformation presented in Figure 1 [6]. After release of the pressure at 5.1 GPa, the initial hcp state was not recovered completely, and the Sm-type domain appeared to survive metastably. In the case of Tb, the decrease in M started at around $P = 2$ GPa, and the change occurred within the hcp phase. Our interpretation of the experimental data is that the disappearance of M is completed after the hcp-Sm structural transition.

For Dy, the magnetic moment began to decrease at around 1 GPa, whereas the hcp was stabilized at pressures up to 4.3 GPa (Fig. 6(c)). In a previous report, the Sm phase was observed experimentally at $P = 7.4$ GPa [17]. The relationship between the decrease of M and structural transition seen for Dy more closely resembles that seen for Tb than that observed for Gd.

As for Ho, the experimental verification of the hcp-Sm transition requires a pressure greater than 10 GPa. Therefore, we refer to the data from previous reports [6]. The hcp-Sm structural transition occurred at around 7 GPa. M began to decreases within the hcp phase, and the disappearance of M was almost complete after transformation to the Sm structure, as seen for Tb and Dy.

From this series of magnetization measurements and XRD studies, we conclude that there is no unifying relationship between the decrease of M and the change in structural symmetry. In the next section, we attempt to uncover the universality on the above-mentioned phenomena.

4 Discussion

We have summarized a series of results for T_C, T_N, M, and V, which were derived using the strategy of Jackson *et al.* [11], who plotted changes in T_C and T_N against a pressure, with normalization for each specified pressure, based on the AC measurements. In the current study, we constructed similar plots for M and V, as well as for T_C (T_N) under pressure. Figure 7 shows the pressure dependencies of T_C (a), M (b), and V (c) using the above normalized pressures against each P_C as the horizontal axis. In this case, P_C is the critical pressure determined by the disappearance of DC magnetization in a high magnetic field. Surprisingly, for both T_C (T_N) and V, the data for Gd-Ho are scaled on a line. This reveals that both the pressure dependence of T_C (T_N) and the disappearance of M are not directly related to the change in structural symmetry, but rather to volume shrinkage. We found that the disappearance of M was completed at a volume shrinkage of about 16.7 ±1.7%. Based on these results, we propose that the magnetic properties of Gd-Ho could be understood within a united band picture, in which the volume becomes a parameter that characterizes the magnetism.

In general, the RKKY interaction is expressed using the following Hamiltonian equation,

$$H_{\mathrm{RKKY}} = -2K_{\mathrm{ij}}\boldsymbol{J}_{\mathrm{i}} \cdot \boldsymbol{J}_{\mathrm{j}}$$

where total angular momentum J_{i} is the sum of orbital angular momentum L_{i} plus the spin angular momentum S_{i} ($J_{\mathrm{i}} = L_{\mathrm{i}} + S_{\mathrm{i}}$). Thus, K_{ij} is the exchange integral:

$$K_{\mathrm{ij}} = -\left(\frac{9\pi}{4N}\right)(g-1)^2 I_{\mathrm{eff}}{}^2 D(E_{\mathrm{F}})F(2k_{\mathrm{F}}R_{\mathrm{ij}}),$$

where $R_{\mathrm{ij}} = |\boldsymbol{R}_{\mathrm{i}} - \boldsymbol{R}_{\mathrm{j}}|$, $D(E_{\mathrm{F}})$ is the density of the states at the Fermi level E_{F}, and k_{F} is the Fermi wave vector. I_{eff} stands for the effective exchange integral between the conduction electron and the localized f-electron, and $F(x)$ represents the spatial distribution of the conduction electron.

The preliminary band calculation reveals that narrowing of the band width of the itinerant s,d hybridized electrons and broadening of the band width of the localized f-orbital electrons play important roles in decreasing the bulk magnetization of Gd under pressure [18].

Next, we compare the magnetism of Gd with that of Europium (Eu), which is just left of Gd in the Periodic Table. Gd exhibits an FM properties, while Eu does not have an FM phase. In theory, a double-exchange interaction due to the d-orbital electron in Gd plays an important role in stabilizing the FM property. We can propose the following model: in the initial state of Gd, the FM double-exchange interaction overcomes the AFM superexchange interaction, while under the pressurized state, the situations of superiority and inferiority are reversed. In any case, it is difficult to explain the present experimental data solely on the basis of the behaviors of the s- and f-orbital electrons. A united theory that interprets a series of effects induced by pressure is desirable.

5 Conclusion

The magnetization measurements at high magnetic fields for Gd, Tb, Dy, and Ho were performed in the pressure region up to 9.2 GPa. Given the results of the magnetization and XRD measurements, it is clear that the pressure dependencies of magnetic ordering temperatures and the disappearance of magnetization for a series of elements are scaled not with the structural phase, but with the volume shrinkage. The present results expand our understanding of itinerant ferromagnets.

<References >

1. M. A. Ruderman and C. Kittel, Phys. Rev. **96**, 99 (1954); T. Kasuya, Prog. Theor. Phys. **16**, 45, 58 (1956); K. Yosida, Phys. Rev. **106**, 893 (1957).

2. A. Jayaraman and R. C. Sherwood, Phys. Rev. Lett. **12**, 22 (1964).

3. Wakabayashi, H. Kobayashi, H. Nagasaki and S. Minomura, J. Phys. Soc. Jpn. **25**, 227 (1968).

4. K. Takemura and K. Syassen, J. Phys. F: Met. Phys. **15**, 543 (1985).

5. J. Akella, G. S. Smith and A. P. Jephcoat, J. Phys. Chem. Solids **49**, 573 (1988).

6. W. A. Grosshans and W. B. Holzapfel, Phys. Rev. B **45**, 5171 (1992).

7. L. B. Robinson, F. Milstein and A. Jayaraman, Rhys. Rev. **134**, A187 (1964).

8. D. B. McWhan and A. L. Stevens, Rhys. Rev. **139**, A682 (1965).

9. J. J. M. FRanse and R. Gersdorf, Rhys. Rev. Lett. **45**, 50 (1980).

10. T. Iwamoto, M. Mito. M. Hidaka, T. Kawae and K. Takeda, Rhysica B **329-333**, 667 (2003).

11. D. D. Jackson, V. Malba, S. T. Weir, P. A. Baker and Y. K. Vohra, Rhys. Rev. B **71**, 184416 (2005).

12. M. Heinemann and W. M. Temmerman, Phys. Rev. B **49**, 4348 (1994).

13. M. Mito, M. Hitaka, T. Kawae, K. Takeda, T. Kitai, and N. Toyoshima, Jpn. J. Appl. Phys. **40**, Part 1, 6641 (2001).

14. M. Mito, J. Phys. Soc. Jpn. **76**, Suppl.A. 182 (2007).

15. G. J. Piermarini, S. Block, J. D. Barnett and R. A. Forman, J. Appl. Phys. **46**, 2774 (1975).

16. A. Fujiwara, K. Ishii, T. Watanuki, H. Suematsu, H. Nakao, K. Ohwada, Y. Fujii, Y. Murakami, T. Mori, H. Kawada, T. Kikegara, O. Shimomura, T. Matsubara, H.

Hanabusa, S. Daicho, S. Kitamura and C. Katayama, J. Appl. Cryst. **33**, 1241 (2000).

17. R. Patterson, C. K. Saw and J. Akella, J. Appl. Physics, **95**, 5443 (2004).

18. M. Tokita, K. Zenmyo, M. Mito, K. Matsumoto and K. Takeda, *J. Magn. Magn. Mater.* **310**, 1738 (2007).

<Figure Legends>

Figure 1

 Structural phase transitions of Gd, Tb, Dy, and Ho under pressure [6].

Figure 2

 Magnetization curves for polycrystalline samples of Gd, Tb, Dy, and Ho at $T = 5$ K

 under ambient pressure. The unit of magnetization M is the Bohr magneton μ_B.

Figure 3

 Temperature dependence of the magnetization values (M) of Gd (a; $H = 0.5$ T), Tb (b;

 $H = 0.3$ T), Dy (c; $H = 0.3$ T), and Ho (d; $H = 0.5$ T). The plotted data do not include

 the background contribution of DAC. The T_C and T_N at ambient pressure are

 represented by arrows.

Figure 4

 Pressure dependencies of the FM transition temperature T_C and the AFM transition

temperature T_N of Gd-Ho. These pressure dependencies are summarized in Table 1.

Figure 5

 Pressure dependence of the maximum value of $M(T)$, M_{max}, for Gd-Ho. The critical

pressure (P_C) levels associated with the disappearance of M are summarized in Table 1.

Figure 6

 Powder X-ray diffraction patterns of Gd, Tb and Dy at room temperature.

The pressures required for structural transition are estimated as: for Gd, P_C (hcp-Sm) = 2.0 ±0.5 GPa, P_C (Sm-dhcp) = 9.0 ±1.0 GPa; and for Tb, P_C (hcp-Sm) = 4.6 ±0.5 GPa. Some of the diffraction peaks are marked with an inverse triangle or asterisk for guidance. The details of the plane indexes are given in the text.

Figure 7

Scaling of T_C and T_N (a), M_{max} (b) and V for Gd-Ho against the pressures normalized for each critical pressure, at which the FM moments disappear.

TABLE 1   dT_C/dP, dT_N/dP, P_C, P_C (hcp-Sm) for Gd, Tb, Dy and Ho.

	dT_C/dP [K/GPa]	dT_N/dP [K/GPa]	P_C [GPa]	P_C (hcp-Sm) [GPa]
Gd	-12.2		9.0	2.0 ±0.5
Tb	-12.6	-11.4	7.5	4.6 ±0.5
Dy	- 7.2	- 1.4	7.6	5.0 (ref.6)
Ho	- 4.1	- 0.15	11.0	7.0 (ref.6)
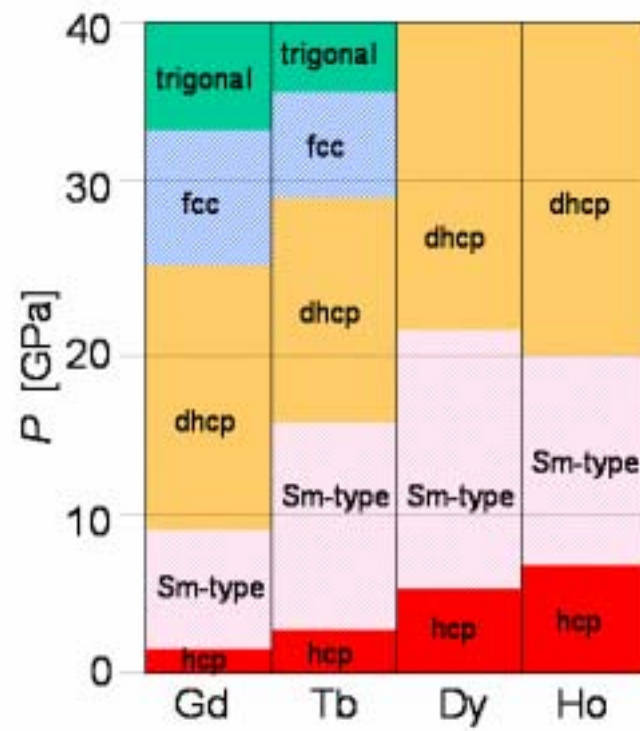
Figure 1

M. Mito et al.
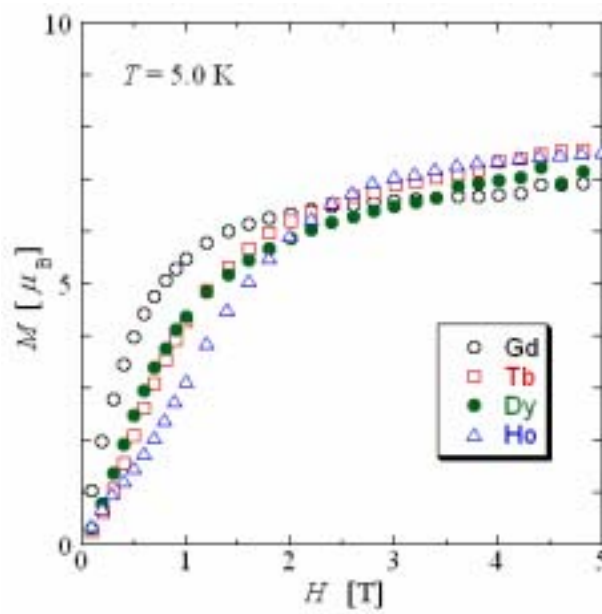
Figure 2

M. Mito et al.
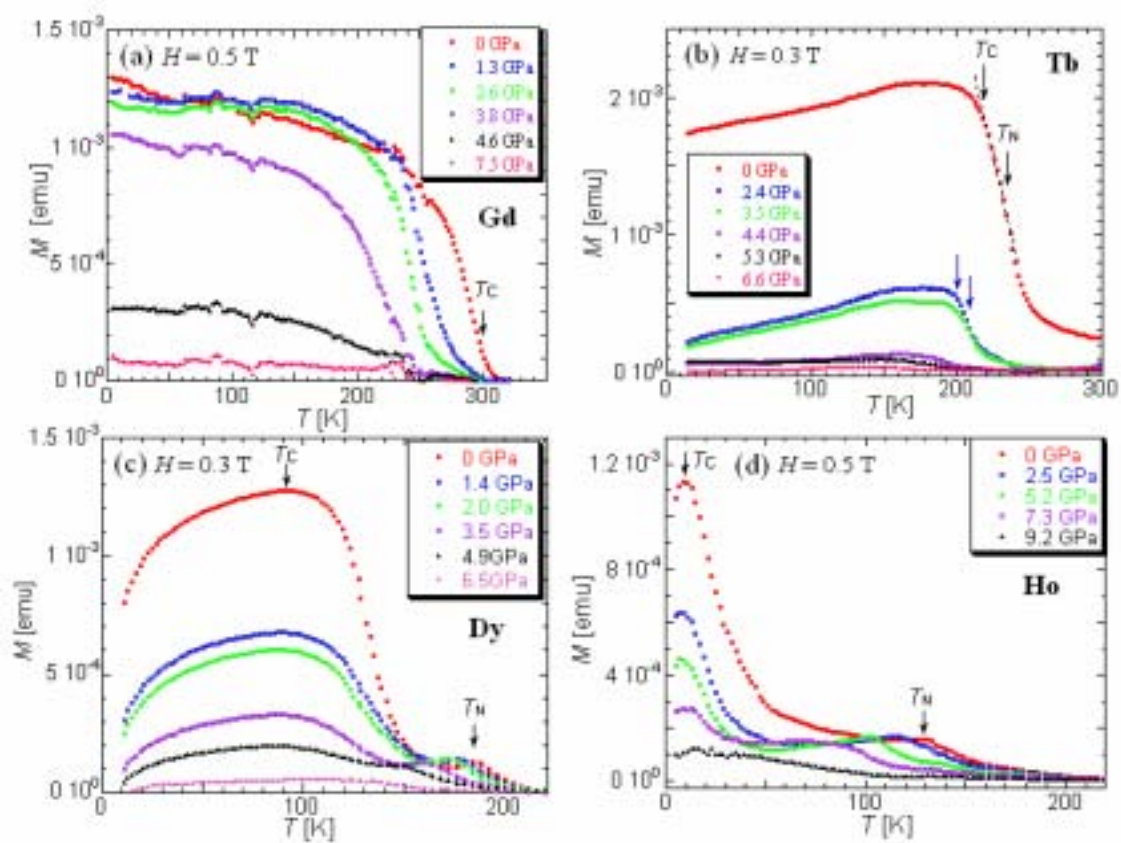
Figure 3

M. Mito et al.
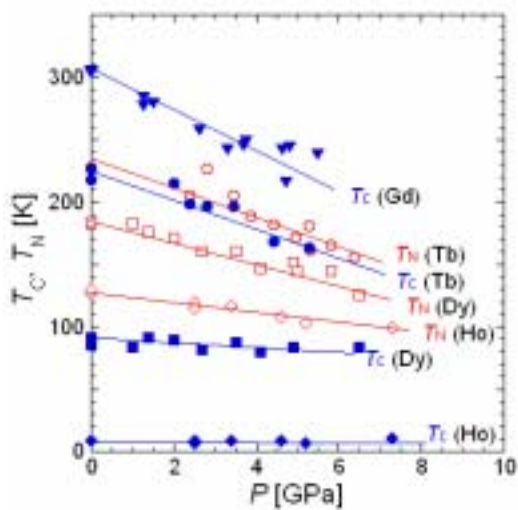
Figure 4

M. Mito et al.
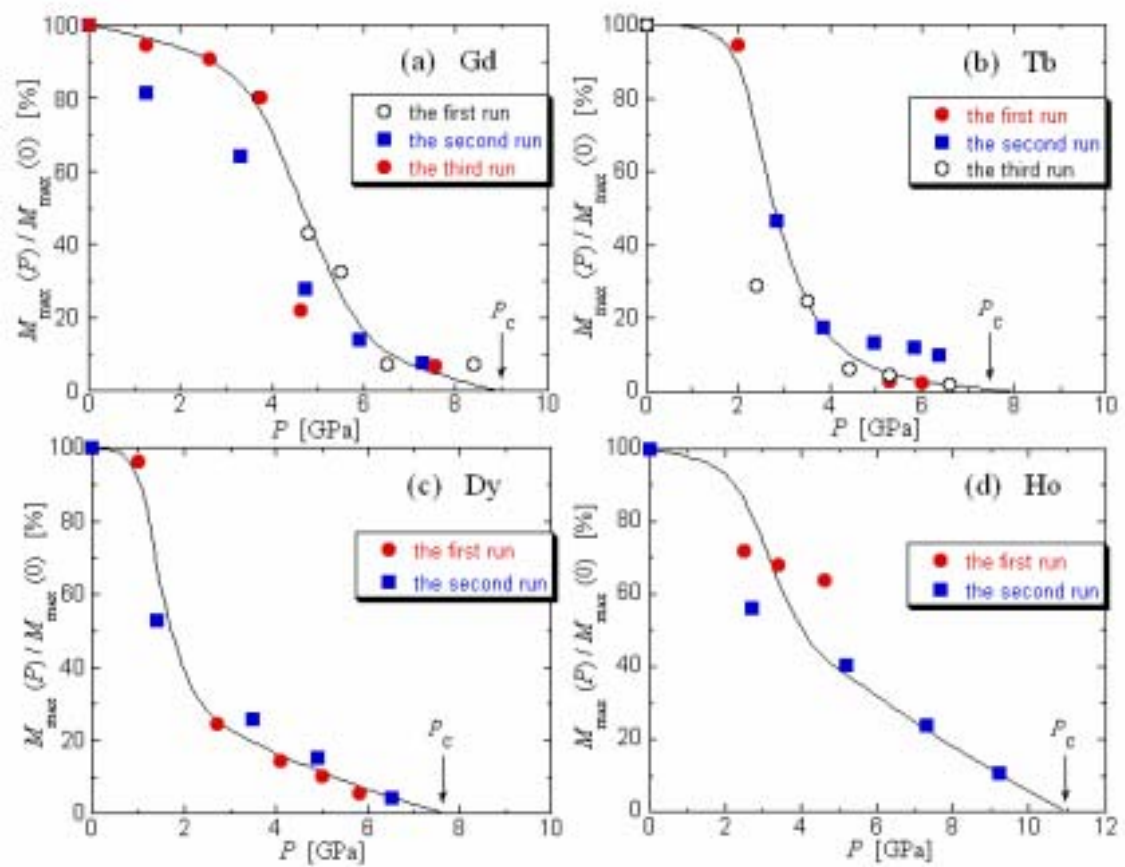
Figure 5

M. Mito et al.
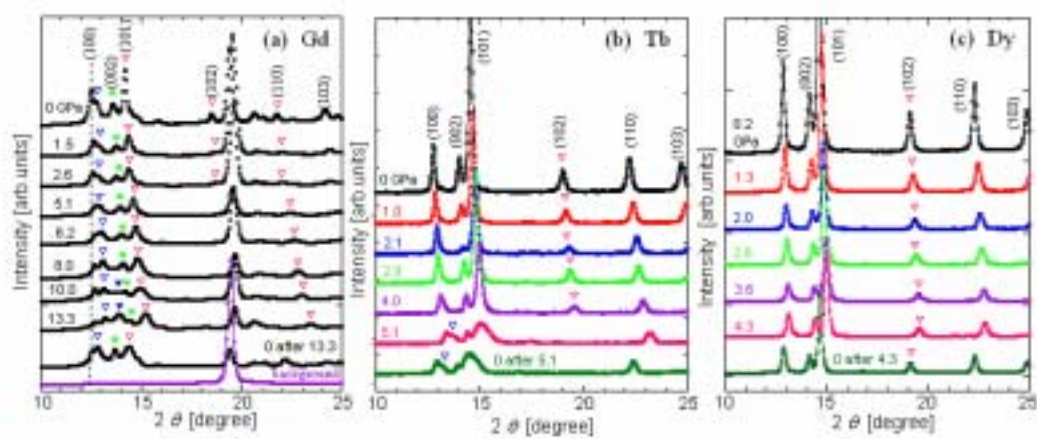
Figure 6

M. Mito et al.

Figure 7

M. Mito et al.